

Electrical Power Generation from Vortex-Induced Vibrations of a Circular Cylinder

A. K. Soti^{1,2,3}, M. C. Thompson², J. Sheridan² and R. Bhardwaj³

¹IITB-Monash Research Academy
IIT Bombay, Mumbai, Maharashtra, 400076, India

²Department of Mechanical Engineering
Monash University, Clayton 3800, Australia

³Department of Mechanical Engineering
IIT Bombay, Mumbai, Maharashtra, 400076, India

Abstract

Renewable energy sources are likely to become essential due to continuously increasing energy demands and depletion of the natural resources that are used for power generation, such as coal and gas. They are also advantageous for their reduced environmental impact. We present a numerical study on the possibility of generating electrical power from vortex-induced vibration (VIV) of a cylinder. The cylinder is free to oscillate in the direction transverse to the incoming flow. The cylinder is attached to a magnet that can move along the axis of a coil made from a conducting wire. The magnet and the coil together make a linear electrical generator. For the simulations reported here, the Reynolds number is kept at 150 so that the flow is laminar and two-dimensional (2D). The incompressible 2D Navier-Stokes equations are solved using an extensively validated spectral-element based solver. We study the effect of the electromagnetic (EM) damping constant ξ_{m0} and coil dimensions (radius a and length L) on the electrical power extracted. We find there is an optimal value of ξ_{m0} ($\xi_{m0,opt}$) at which maximum electrical power is generated. As we increase either the radius or the length of the coil, the value of $\xi_{m0,opt}$ is observed to increase. Although the maximum average power remains the same, a larger coil radius or length results in a more favourable system which can extract a relatively large amount of power when ξ_{m0} is far from $\xi_{m0,opt}$.

Introduction

A bluff body kept in free-stream flow gives rise to a well known phenomenon called ‘‘vortex shedding’’. Vortices are shed periodically from the bluff body, which results in a fluctuating lift force on the body. If the body is free to move along transverse direction then the fluctuations in lift force can cause the body to oscillate. This is referred to as ‘‘Vortex-Induced Vibration (VIV)’’. A lot of work has been done in the past on VIV of circular cylinders, for example, refer to the reviews [1, 8, 10]. The transverse displacement of the body varies almost, but not exactly, in a sinusoidal fashion with time [11], and the amplitude of the response is divided into three categories: initial, upper and lower branch [5]. The amplitude depends on the mass-damping parameter ($m\xi$) and the Reynolds number.

The oscillation of a bluff body due to fluid flow is an opportunity to harness flow energy. It can be done by mounting the body on a piezoelectric transducer so that the motion of the body results in deformation of the piezoelectric material and thereby produces some electrical charge [3]. In reference [2] a new device called VIVACE converter was proposed to convert flow energy into electricity using VIV of a cylinder. In the present work, we focus on another method for harnessing flow energy by using a linear electromagnetic alternator attached to the body. The linear alternator comprises a magnet and conducting coil. The

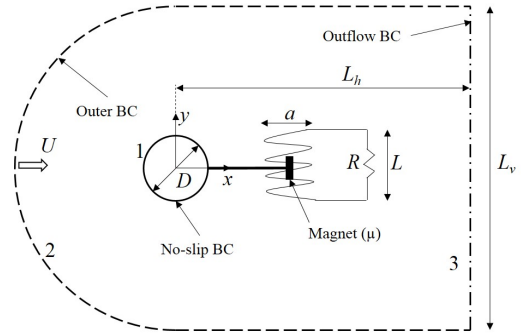


Figure 1: Problem sketch and boundary conditions.

magnet or the coil can be attached to the body. When the body undergoes VIV, the relative motion between the magnet and coil creates a voltage across the coil that is connected to a resistive load. By Lenz’s law, induced current in the coil applies a retarding force to the magnet. Effectively, the linear generator applies a damping force on the body with a spatially varying damping coefficient. In the present work, we find out the maximum power that can be extracted by such a system. We also study the effects of length and radius of the coil on the performance of the system.

Problem definition and methodology

We consider a vertical elastically mounted circular cylinder of diameter D kept in free-stream flow with velocity U . The cylinder is free to move only in transverse (y) direction, with the cylinder displacement denoted by y . The cylinder is attached to a magnet with dipole moment μ . The mass-ratio of cylinder-magnet assembly is m . The magnet can move inside a conducting coil of radius a and length L . The coil is connected to a load resistance R . The computational domain is shown in figure 1. The Reynolds number $Re = UD/\nu$, where ν is the kinematic viscosity, is taken as 150, which enables us to make the assumption of two-dimensional (2D) flow. The fluid flow is governed by the following non-dimensional Navier-Stokes equation

$$\frac{\partial \mathbf{u}}{\partial t} + (\mathbf{u} \cdot \nabla) \mathbf{u} = \nabla p + \frac{1}{Re} (\nabla^2 \mathbf{u}) + \mathbf{a}_F, \quad (1)$$

where \mathbf{a}_F represents the acceleration of the reference frame, which is chosen to be the frame of the cylinder in the present case. Here, \mathbf{u} and p denotes the fluid velocity vector and pressure, respectively. The size of the computational domain is taken as $L_h = 25D$ and $L_v = 40D$. The x -component of flow velocity is prescribed as U at the inlet, top and bottom boundaries (2) and the y -component is prescribed as the transverse

velocity of the cylinder. The cylinder surface (1) is considered to be a no-slip boundary and Neumann boundary condition is applied at the outlet (3).

As the cylinder undergoes VIV, the attached magnet can generate a voltage across the coil due to Faraday's law of electromagnetic induction. If the coil is connected to a load resistance R then it can oppose the motion of the magnet by applying a retarding force which is proportional to the velocity of the magnet relative to the coil. Hence, the electromagnetic (EM) generator can be modelled as a damper with the following non-dimensional expression for the force applied to the cylinder

$$F_m = 2\pi^2 m \xi_{m0} g^2 f_n \dot{y}, \quad (2)$$

where \dot{y} and f_n represents the velocity and natural frequency of the cylinder, respectively. The parameter $\xi_{m0} = c_{m0}/c_c$ is an EM damping constant which controls the amount of damping in the system where $c_{m0} = \mu^2/(RD^4)$, and c_c is the critical damping of the system. The function $g = g(y(t))$ dictates the spatial variation of the damping ratio and is given by the following expression [4]

$$g = \left(\frac{2\pi N a^2}{L} \right) \left[\frac{1}{(a^2 + (y_{cm} - L/2)^2)^{3/2}} - \frac{1}{(a^2 + (y_{cm} + L/2)^2)^{3/2}} \right], \quad (3)$$

where y_{cm} is the distance between the magnet and the centre of the coil. The number of turns in the coil are N . Finally, the motion of the cylinder is governed by the following non-dimensional equation

$$\ddot{y} + 4\pi(\xi + \xi_m) f_n \dot{y} + 4\pi^2 f_n^2 y = \frac{2 C_L}{\pi m}, \quad (4)$$

where y , \dot{y} and \ddot{y} denote the cylinder displacement, velocity and acceleration in the transverse direction, C_L is the lift coefficient. ξ represents the structural damping ratio and $\xi_m = \xi_{m0} g^2$ is the EM damping ratio. The non-dimensional reduced velocity is defined as $U_r = U/(f_n D)$ where f_n is the natural frequency of the cylinder-magnet assembly in the fluid. The added-mass coefficient for finding f_n is assumed 1 for the present study. The electrical power P can be calculated by multiplying the EM damping force (F_m) with the cylinder velocity.

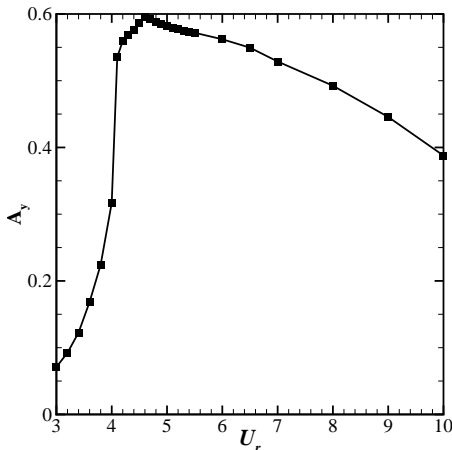


Figure 2: Maximum oscillation amplitude versus non-dimensional reduced velocity for $m = 1$ and $Re = 150$.

We use a Galerkin-based spectral element solver to simulate the process of energy extraction from VIV of the circular cylinder. Please refer to [6, 9] for details of the numerical method. The details of the mesh used for the simulations and grid independence study are provided in [6, 7].

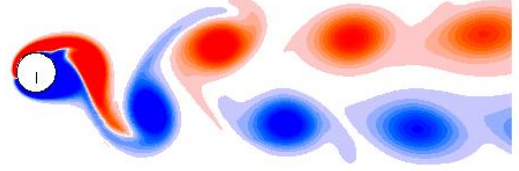


Figure 3: Vorticity contours for $m = 1$, $Re = 150$, $\xi_{m0} = 4.0 \times 10^{-5}$, $a = 0.6$, $L = 0.6$ and $U_r = 5.3$. The scale is from -2 to 2.

Results and Discussion

To demonstrate that electrical energy can be harnessed from VIV of a circular cylinder, we take a cylinder-magnet system with mass ratio $m = 1$. The Reynolds number is kept at 150. The non-dimensional coil dimensions are taken as $a = 0.6$ and $L = 0.6$. In later sections, we will study the effects of these parameters. In figure 2 we have plotted the maximum amplitude of the cylinder at zero damping for various values of U_r . We can see the initial and lower branches in the response curve. The largest amplitude is achieved for the values of U_r between 4.5-5.

Energy Extraction

In figure 3 we show the vorticity contours for a typical case. The parameters for this case corresponds to maximum power extraction situation, as discussed later in this section. Two vortices are shed periodically during a cycle of oscillation of the cylinder. This is referred to as 2S vortex shedding mode in literature.

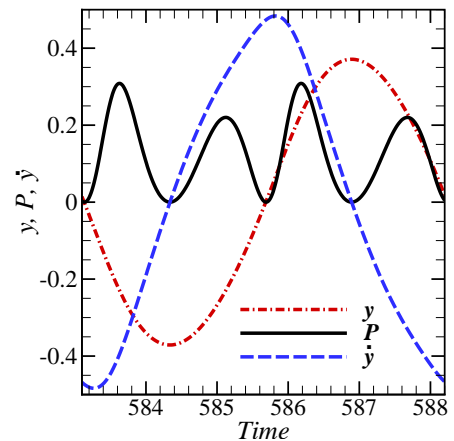


Figure 4: Time variation of cylinder displacement, velocity and power for $m = 1$, $Re = 150$, $\xi_{m0} = 4.0 \times 10^{-5}$, $a = 0.6$, $L = 0.6$ and $U_r = 5.3$.

In figure 4 we plot the temporal variation of power, transverse displacement and velocity of the cylinder. The displacement and velocity curves are not sinusoidal due to the spatially varying nature of the EM damping. Also, the instant of maximum velocity does not coincide with the instant when the displacement is zero. The power curve has two types of local maxi-

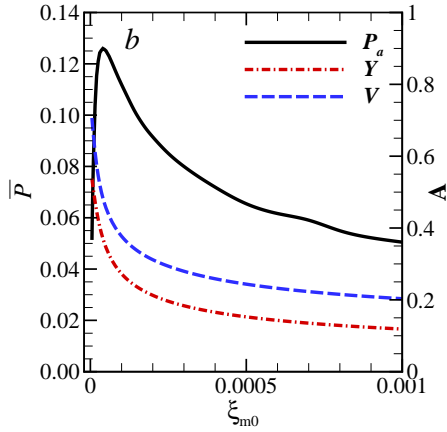


Figure 5: Variation of average power (left) and displacement and velocity amplitudes (right) with ξ_{m0} for $a = 0.6, L = 0.6$ and $U_r = 5.3$.

mum. The first and second maximum occur when the cylinder is moving away and towards its mean position, respectively. This happens because the function g has two maximum at equal distance from mean position ($y = 0$). Notice that the magnitude of first maximum (0.31) is greater than that of the second one (0.22). The reason is the fact that the cylinder displacement and velocity are not sinusoidal. Both the maximum occur when $y = \pm 0.23$ but the cylinder velocities at the instance of first and second maximum are 0.39 and 0.33, respectively. The frequency of power is twice that of oscillation of the cylinder.

The variation of average power calculated over a cycle of os-

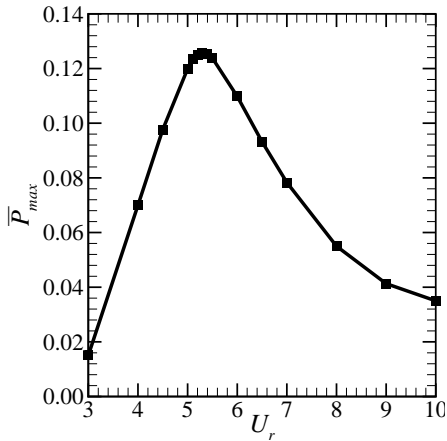


Figure 6: Variation of maximum average power with U_r at $Re = 150$ for $a = 0.6, L = 0.6$ and $m = 1$.

cillation with the EM damping constant is shown in figure 5. We also show the variation of displacement and velocity amplitudes of the cylinder. As expected, the displacement and hence the velocity amplitude of the cylinder decreases monotonically with ξ_{m0} . Since the power is the product of EM damping force and the cylinder velocity, there should be an optimal value of ξ_{m0} at which maximum electrical power is produced. This is what we see in figure 5 where $\xi_{m0,opt} = 4.0 \times 10^{-5}$. The maximum average power is $\bar{P}_{max} = 0.126$. The corresponding optimal amplitudes of displacement and velocity are 0.37 and 0.48, respectively. In figure 6 we show the variation of maximum average power (\bar{P}_{max}) with reduced velocity. The peak value of \bar{P}_{ma} is obtained at $U_r = 5.3$.

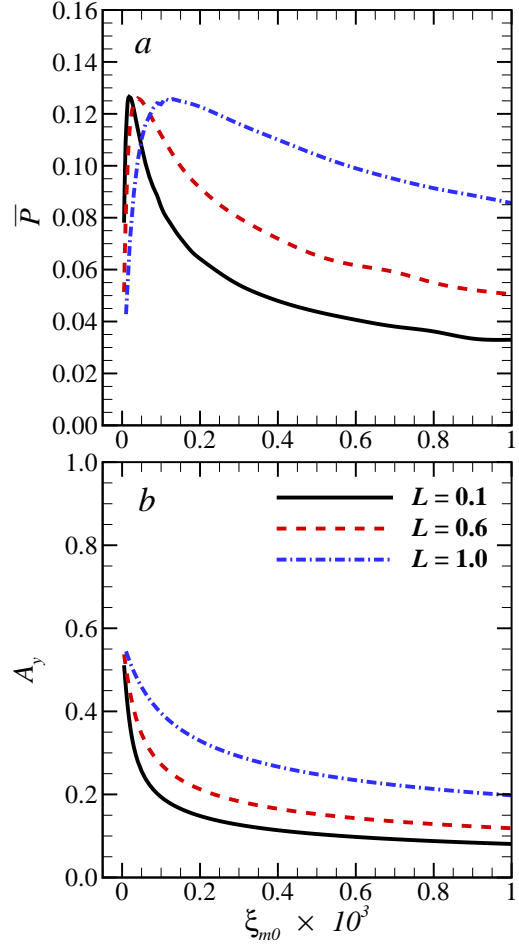


Figure 7: Variation of (a) average power and (b) displacement amplitude with ξ_{m0} for $m = 1, a = 0.6$, and $U_r = 5.3$.

Effect of Length of the Coil

In this section we describe the effect of length of the coil on the amount of power extracted. For this, we vary the value of L to 0.1 and 1.0, in addition to the value of 0.6 already investigated. Other parameters are kept same. The variation of average power (\bar{P}) and displacement amplitude (A_y) with ξ_{m0} for three values of L is shown in figure 7. The maximum average power is almost unaffected by the coil length. As the value of L increases, we see a decrease in the rate at which the average power decays with ξ_{m0} . The same is true for the displacement amplitude of the cylinder. The optimal displacement amplitudes for $L = 0.1, 0.6$ and 1.0 are 0.38, 0.37 and 0.39, respectively. If we plot \bar{P} against A_y (not shown here) then all three cases approximately collapse to a single curve which suggests that maximum power is strongly dependent on the oscillation amplitude and it is not directly dependent on the nature of damping. On the other hand, a larger value of L provides a more advantageous system in the sense that the system can provide a significant amount of power even when it is not close to its optimal operating condition.

Effect of Radius of the Coil

Now we discuss the effect of the radius of the coil on average harnessed power. This time, we vary the value of a to 0.4 and 0.8, in addition to the value of 0.6 already considered. We plot the average power and displacement amplitude of the cylinder for three values of a in figure 8. The effect of a is similar to that of L . The maximum average power is unaffected by a but

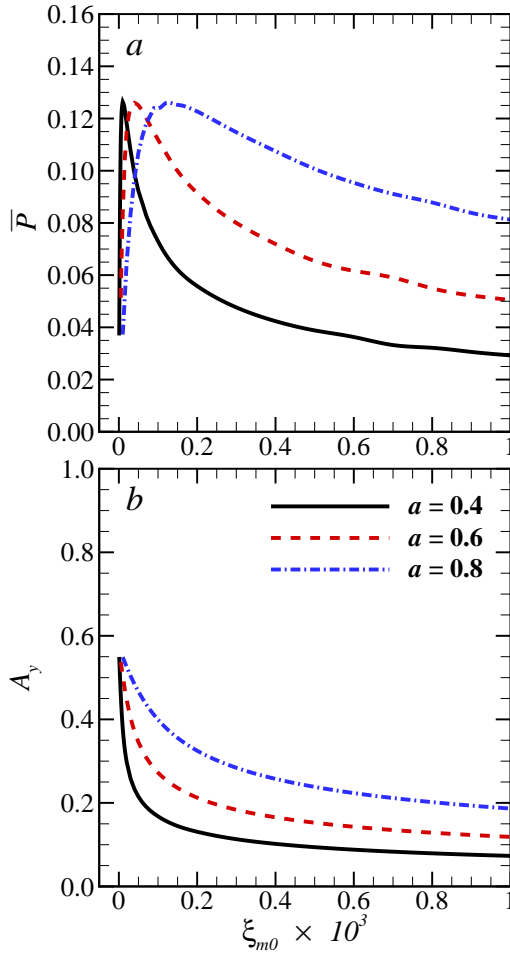


Figure 8: Variation of (a) average power and (b) displacement amplitude with ξ_{m0} for $m = 1$, $L = 0.6$, and $U_r = 5.3$.

the rate of change of \bar{P} with ξ_{m0} decreases with increase in a . The same is seen for the displacement amplitude. The optimal displacement amplitudes for $a = 0.4$, 0.6 and 0.8 are 0.38 , 0.37 and 0.38 , respectively. This supports our point about average power being directly depending on the oscillation amplitude and not the nature of damping.

Conclusions

We demonstrated that some part of flow energy can be converted to electrical energy using vortex-induced vibrations of a circular cylinder. A spectral-element based solver was utilized to simulate the fluid-solid interaction between flow and the cylinder. A linear alternator consisting of a magnet and a coil was used to convert the kinetic energy of the oscillating cylinder into electrical energy. We found that there is an optimal value of electromagnetic damping constant and corresponding oscillation amplitude at which maximum power is extracted. At $Re = 150$, the non-dimensional optimal displacement amplitude is close to 0.37 and is not equal to its maximum possible value at zero damping. The non-dimensional value of maximum average power is 0.13 .

Acknowledgements

The computing time from the MonARCH (Monash Advanced Research Computing Hybrid) is gratefully acknowledged.

References

- [1] Bearman, P., Circular cylinder wakes and vortex-induced vibrations, *Journal of Fluids and Structures*, **27**, 2011, 648–658.
- [2] Bernitsas, M. M., Raghavan, K., Ben-Simon, Y. and Garcia, E., Vivace (vortex induced vibration aquatic clean energy): A new concept in generation of clean and renewable energy from fluid flow, *Journal of Offshore Mechanics and Arctic Engineering*, **130**, 2008, 041101.
- [3] Dai, H., Abdelkefi, A., Yang, Y. and Wang, L., Orientation of bluff body for designing efficient energy harvesters from vortex-induced vibrations, *Applied Physics Letters*, **108**, 2016, 053902.
- [4] Donoso, G., Ladera, C. and Martin, P., Magnetically coupled magnet–spring oscillators, *European Journal of Physics*, **31**, 2010, 433.
- [5] Khalak, A. and Williamson, C., Motions, forces and mode transitions in vortex-induced vibrations at low mass-damping, *Journal of Fluids and Structures*, **13**, 1999, 813–851.
- [6] Leontini, J., Stewart, B., Thompson, M. and Hourigan, K., Predicting vortex-induced vibration from driven oscillation results, *Applied Mathematical Modelling*, **30**, 2006, 1096–1102.
- [7] Leontini, J., Stewart, B., Thompson, M. and Hourigan, K., Wake state and energy transitions of an oscillating cylinder at low Reynolds number, *Physics of Fluids (1994-present)*, **18**, 2006, 067101.
- [8] Sarpkaya, T., A critical review of the intrinsic nature of vortex-induced vibrations, *Journal of Fluids and Structures*, **19**, 2004, 389–447.
- [9] Thompson, M., Hourigan, K. and Sheridan, J., Three-dimensional instabilities in the wake of a circular cylinder, *Experimental Thermal and Fluid Science*, **12**, 1996, 190–196.
- [10] Williamson, C. and Govardhan, R., Vortex-induced vibrations, *Annual Review of Fluid Mechanics*, **36**, 2004, 413–455.
- [11] Zhao, J., Nemes, A., Jacono, D. L. and Sheridan, J., Comparison of fluid forces and wake modes between free vibration and tracking motion of a circular cylinder, in *18th Australasian Fluid Mechanics Conference*, Australasian Fluid Mechanics Society, 2012.